

PATTERN FORMATION IN A CELLULAR SLIME MOLD

H. G. OTHMER*, B. LILLY* , AND J. C. DALLON†

Abstract. Stream formation is a prominent feature of aggregation in the cellular slime mold *Dictyostelium discoideum*, but there is no commonly-accepted explanation for this and existing models make different predictions as to how it originates. In this paper we discuss the relationship between cell-based and continuum descriptions of aggregation and the origin of streaming in these two types of models.

Key words. Chemotaxis, aggregation, pattern formation, streaming

1. Introduction. The social amoeba *Dictyostelium discoideum* (Dd) is a model developmental system that employs many of the basic processes used during the development of higher organisms at various stages of its life cycle. These include detection of extracellular signals and their transduction into an intracellular signal that activates processes such as signal relay and gene expression, oriented cell movement toward a signal, movement either as a single cell or as part of a tissue-like aggregate, differentiation of a genetically-identical population into several distinct cell types, and regulation of the proportions of these cell types over a wide range of total cell number. These cells normally feed on bacteria [2], but upon starvation they express surface receptors for detecting the messenger molecule cyclic adenosine monophosphate (cAMP) and develop the ability to relay cAMP signals [9]. After about eight hours, randomly-located cells called pacemakers start to emit cAMP periodically [27], and surrounding cells move towards the cAMP source and relay the cAMP signal to more distant cells. Eventually the entire population collects into mound-shaped aggregates containing up to 10^5 cells. The mound then elongates into a cylindrical shape, which topples over and migrates as a cigar-shaped slug for up to twenty four hours. During the late mound stage and the migration period the cells start to differentiate into prestalk and prespore cells. Differentiation initially occurs in randomly-located cells in the late mound stage, but later a combination of cell sorting and signaling by cells in the tip results in the spatial separation of cell types, with prestalk cells in the anterior fourth of the slug and prespore cells in the posterior three fourths of the slug. When conditions are favorable, the tip of the slug is extended upwards and a fruiting body comprising a spherical cap of spore cells supported by a stalk is formed. The spores remain dormant until conditions for germination are favorable, whereupon they are dispersed and the cycle begins anew.

*Department of Mathematics, University of Utah, Salt Lake City, UT, Supported by NIH Grant GM 29123.

†Department of Mathematics, Heriot Watt University, Edinburgh, UK, Supported by EPSRC Grant GR/K71394.

The autonomous production and relay of cAMP pulses by individual cells organizes chemotactic aggregation, the transformation of mounds into slugs, the migration of slugs over the substratum, and the culmination into fruiting bodies. The regulation of the enzyme adenylyl cyclase, which produces intracellular cAMP, and the degradation of cAMP by intra- and extracellular cAMP phosphodiesterases (PDEs) are the major components of oscillatory signaling. Experimental progress in understanding the regulation of both enzymes at the biochemical level has been accompanied by the formulation of theoretical models describing the dynamics of the system. Adaptation of cAMP production, by which we mean that it eventually returns to basal level in the presence of constant cAMP stimuli, is essential for oscillatory signaling and for relay during aggregation. The observables during the relay response are the intracellular cAMP, the secretion rate, and the morphology of the cell. Early studies showed that the relay response adapts, but this response is the end result of numerous intracellular steps. However, if PDE is not regulated then termination of the relay response requires that the rate of cAMP production returns to the basal level, and hence that either the activity of adenylyl cyclase or a component upstream of it adapts. The current state of our experimental and theoretical understanding of cAMP signaling in *Dd* is reviewed in Othmer and Schaap [22], which is referred to as OS hereafter. In the following section we briefly describe a theoretical model that captures much of the known behavior of this system and in subsequent sections we turn to the main topics, which are the relationship between continuum and cell-based models, and how streaming during aggregation is initiated.

2. A theoretical model for signal transduction, relay and oscillations in *Dd*. Experimental results reviewed in OS show that models of the transduction/relay system in which the rates of change of intracellular state variables depend only on the present state of the system must incorporate at least two intracellular variables, one of which adapts in the sense used previously, and one which effects the adaptation but itself does not return to its pre-stimulation level. Certainly the primary intracellular variable should be cAMP, but the second intracellular variable in such a minimal model is not easily determined. At present a model developed by Tang and Othmer [34, 35] incorporates the most biochemical detail of the signal transduction process and reproduces the input-output behavior of cells most accurately, although there are details that it does not capture. The model incorporates three major pathways in the transduction of and adaptation to an extracellular cAMP signal. First, there is a stimulus pathway in which cAMP binds to surface receptors which then catalyze the activation of an intracellular stimulatory G-protein. This in turn binds with the inactive form of adenylyl cyclase and produces the activated form of the enzyme. Second there is a pathway in which an inhibitory G-protein is produced by analogous steps, and this G-protein inhibits the first path-

way. Finally, in the pathway for the production and secretion of cAMP, the activated enzyme catalyzes the production of intracellular cAMP ($cAMP_i$), which is then either hydrolyzed by intracellular phosphodiesterase ($iPDE$) or secreted into the extracellular medium ($cAMP_o$).

This kinetic scheme leads to a large system of differential equations, but by scaling and singular perturbation arguments the network and equations can be reduced to five primary variables. The major steps are shown in Figure 1. Details of how this reduction is done can be found in the original papers, where the reduction was done in two steps, first to eight variables [34] and then to five [35]. In the reduced scheme shown in this figure there are four internal variables and one extracellular variable. The components of primary interest in the following equations are the intra- and extracellular cAMP, and these are denoted by C_i and C_o , respectively. The variables w_i , $i = 1,2,3$ represent intermediate species in the signal transduction pathway, as shown in Figure 1. In the following equations Greek letters and lower case c 's represent biochemical parameters, many of which can be obtained from the literature, but the remainder must be estimated [34].

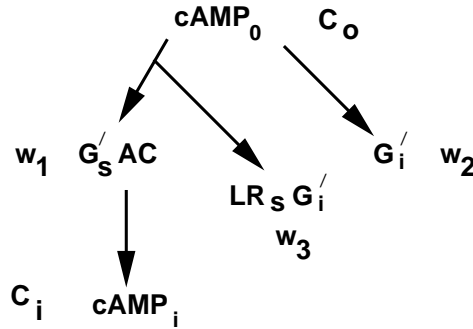


FIG. 1. The reduced network for the five primary variables in the Tang-Othmer scheme. L denotes the ligand ($cAMP_o$) and R_s denotes the receptor in the stimulatory pathway. The symbol beside a species corresponds to the symbol used in (2.1).

$$\begin{aligned}
 \frac{dw_1}{d\tau} &= \alpha_4 u_2 (1 - w_1) - w_1 \\
 \frac{dw_2}{d\tau} &= \beta_2 \beta_3 c_2 u_4 (1 - w_2 - c_3 w_3) - \beta_5 w_2 + \beta_6 c_3 w_3 - c_3 \beta_4 u_1 w_2 \\
 (2.1) \quad \frac{dw_3}{d\tau} &= -(\beta_5 + \beta_6) w_3 + \beta_4 u_1 w_2 \\
 \frac{dC_i}{d\tau} &= \gamma_1 \gamma_2 w_1 + \Gamma_5 (1 - \Gamma_7 w_1) - \gamma_4 \frac{C_i}{C_i + \gamma_3} - sr(C_i) \\
 \frac{dC_o}{d\tau} &= \frac{\rho}{1 - \rho} \left(sr(C_i) - \gamma_7 \frac{C_o}{C_o + \gamma_6} - \gamma_9 \frac{C_o}{C_o + \gamma_8} \right).
 \end{aligned}$$

In these equations the quantities u_i , which arise from singular perturbation of the full equations, are given by

$$u_1 = \frac{\alpha_0 C_o + (\beta_5 - \alpha_0 C_o) w_3}{\alpha_1 + \alpha_0 C_o + \beta_4 w_2}$$

$$u_2 = \frac{\alpha_2 \alpha_3 c_1 u_1 (1 - w_1)}{1 + \alpha_4 + \alpha_2 \alpha_3 c_1 u_1 - \alpha_4 w_1}$$

$$u_4 = \frac{\beta_0 C_o}{\beta_1 + \beta_0 C_o}.$$

A qualitative description of how an extracellular change in cAMP leads to both stimulation of the enzyme and production of cAMP, as well as adaptation to a constant extracellular stimulus, can be found in OS. Simulations of these equations show that the model can reproduce the experimentally-observed behavior, both when extracellular cAMP is a prescribed function of time, as in perfusion experiments, and when it is one of the system variables, as in the above equations. In essence the model can reproduce the input-output behavior of individual cells quite well, and thus it can be used to study questions that only depend on biochemical fidelity at this level. Most of these concern aspects of aggregation and later development.

Aggregation following starvation begins when individual cells or groups of cells begin signaling by releasing cAMP periodically. Nearby cells sense this signal and respond to it either by moving toward the source of the signal, or by both relaying the signal and moving toward its source, depending on whether they are only competent for chemotaxis or competent for both relay and chemotaxis. If relay-competent Dd cells are spread over an agar surface, two-dimensional waves of cAMP can be observed [36, 18, 8]. The waves of extracellular cAMP travel across the field in the form of either target patterns (expanding concentric waves), or spiral waves with rotating cores. Different types of interacting wave patterns are observed experimentally, one example of which is shown in Figure 2. The extracellular cAMP wave rises from a level of less than $\sim 10^{-9}$ M to a peak value of $10^{-7} - 10^{-6}$ M in a medium with a cell density of 10^6 cells/cm². In either a spiral wave or a concentric wave, the distance between two traveling fronts is 1–4mm. The speed of these waves is $\sim 300 - 600$ μ m/min, and the time between two successive wave fronts is 6-10 minutes [36, 30]. The traveling cAMP waves serve as the chemotactic signal to induce aggregation of the cells, which move toward the center at about 10–15 μ m/min [40, 39, 6].

Important questions that must be answered to understand the macroscopic behavior of the system include the following.

1. Can individual cells be pacemakers and initiate traveling waves under normal conditions of early aggregation, or is it necessary for two or more cells to come into close proximity in order to initiate a wave?

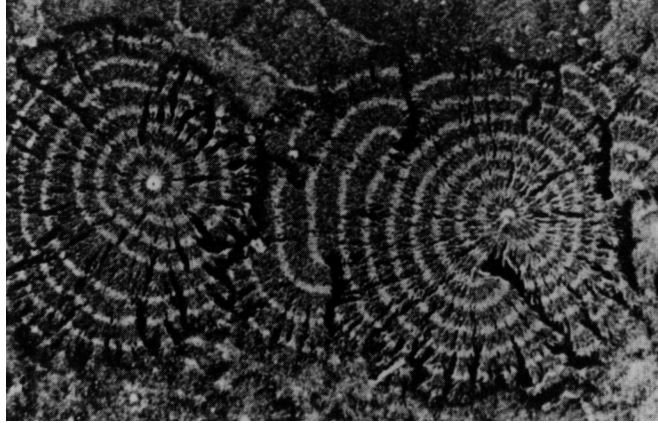


FIG. 2. An example of the wave patterns observed during the aggregation of *Dd*. The light bands represent cells that are moving while the dark bands represent stationary cells. From Newell [18].

2. What determines whether the traveling waves of $cAMP_o$ are axisymmetric target patterns or spiral waves?
3. What are the details of the signal seen by a cell (front-to-back $cAMP$ ratio, etc.), how do cells orient themselves in a traveling wave, and how do they solve the 'back-of-the-wave' problem? Do cells measure spatial gradients, temporal gradients, both, or neither in determining how to move?
4. How accurately must cells determine the optimal direction of movement, or said otherwise, how sloppy can they be in the choice of direction and still aggregate effectively?
5. How should the rules for individual movement, primarily the choice of direction and speed of movement, be incorporated in a continuum description of aggregation?

A review of what is presently known about these questions is given in OS; in the remainder of this paper we focus on two aspects: (i) the connection between continuum and cell-based models, and (ii) the origin of streaming in aggregation.

3. Continuum and cell-based descriptions of wave propagation, cell motion and aggregation.

3.1. Continuum descriptions. Two main approaches are used for describing aggregation and the spatio-temporal patterns that wave propagation and cell movement produce: those in which the cell distribution is treated as a continuum and described by a density function, and those in which the discrete nature of cells is incorporated. Both must use some description of cell motion, and therefore we describe this briefly.

In the absence of cAMP stimuli, Dd cells extend pseudopods in random directions, but aggregation-competent cells respond to cAMP stimuli with characteristic changes in their morphology. Under uniform elevation of the ambient cAMP the early ‘cringe’ response is followed by extension of pseudopods in various directions, and an increase in the motility [39, 42]. A localized application of cAMP elicits the cringe response followed by a localized extension of a pseudopod near the point of application of the stimulus [33]. This type of stimulus is similar to what a cell experiences in a cAMP wave, but cells also respond to static gradients of cAMP. Fisher *et al.* [6] show that cells move faster up a cAMP gradient than down, and that the majority of turns made by a cell are spontaneous. However, the magnitude and direction of a turn is strongly influenced by the gradient in that there is a strong tendency to lock onto the gradient.

In a continuum description of cell motion, movement in the absence of a cAMP stimulus is usually described as an uncorrelated, unbiased random walk of noninteracting particles, and thus this component of motion is described by a diffusion process. In the presence of cAMP gradients such as exist in a passing wave, the simplest description of cell motion is obtained by adding to the diffusive flux a directed component to obtain

$$(3.1) \quad \mathbf{j} = -D_c \nabla \rho + \rho \mathbf{u}_c$$

where \mathbf{u}_c is the macroscopic chemotactic velocity. Patlak [24] was the first to relate the chemotactic velocity to properties of individual cells using kinetic theory arguments to express \mathbf{u}_c in terms of averages of the velocities and run times of individual cells. Alt [1] also used the kinetic theory approach and showed that the flux is approximately given by

$$(3.2) \quad \mathbf{j} = -D_c \nabla \rho + \rho \chi(c) \nabla c$$

$$(3.3) \quad = -D_c \nabla \rho + \rho \nabla \Phi(c)$$

where c denotes the concentration of the chemotactic substance and Φ is a primitive of χ . The function $\chi(c)$ is called the chemotactic sensitivity, and the chemotactic velocity is given by

$$(3.4) \quad \mathbf{u}_c = \chi(c) \nabla c = \nabla \Phi(c).$$

When $\chi > 0$ the tactic component of the flux is in the direction of ∇c and the taxis is positive.

The earliest continuum description of Dd aggregation was proposed by Keller and Segel [12]. Since little was known about signal transduction at that time, their model involved only two variables, the cell density and the cAMP concentration. In this model the cell flux was described by (3.2) and the parameters were tuned to produce a chemotaxis-driven instability of the uniform cell density. This can produce aggregation, but it is now known that aggregation is organized by pacemaker cells that are randomly-distributed in the aggregation field, as was mentioned earlier.

Models based on (3.2) for the cell flux also ignore another key feature of Dd aggregation. It is observed experimentally that wild-type cells only move in the rising phase of the cAMP wave, but if cells predicate motion solely on the cAMP gradient they would move forward as a wave approaches, but then turn around as the wave passes. Continuum descriptions can be modified to incorporate this observation by incorporating adaption to the extracellular cAMP in such a way that cells only move in response to rising concentrations. A detailed scheme for accomplishing this will be described later, but one could simply postulate that the flux relation takes the form

$$(3.5) \quad \mathbf{j} = -D_c \nabla \rho + \rho \chi(c_t) \nabla c$$

where c_t denotes the time derivative of c . If $\chi(c_t) = 0$ when $c_t \leq 0$, then this relation predicts that the chemotactic component of the flux vanishes when the attractant field is locally non-increasing, as it should.

A generalization of this in which c_t is replaced by an intermediate variable has been used by Höfer *et al.* [11]. These authors propose the following simplified model for the aggregation process

$$(3.6) \quad \frac{\partial n}{\partial t} = \nabla \cdot (\mu \nabla n - \chi(v) n \nabla u)$$

$$(3.7) \quad \frac{\partial u}{\partial t} = \lambda [\phi(n) f_1(u, v) - (\phi(n) + \delta) f_2(u)] + \nabla^2 u$$

$$(3.8) \quad \frac{\partial v}{\partial t} = -g_1(u)v + g_2(u)(1 - v).$$

Here n , u and v denote cell density, extracellular cAMP concentration and fraction of active cAMP receptors, respectively. The authors postulate that the magnitude of the chemotactic response depends on the sensitivity of a cell to cAMP, as measured by the fraction of active cAMP receptors, and thus assume that the chemotactic sensitivity has the form

$$\chi(v) = \chi_0 \frac{v^m}{N^m + v^m}, \quad m > 1.$$

They also use simplified versions of the kinetic terms in the Martiel & Goldbeter model [16], and assume that the dependence of the rates of synthesis and degradation on the cell density takes the form $\phi(n) = n/(1 - \rho n/(K + n))$.

When simulated numerically, this continuum model yields aggregation patterns like those observed experimentally (see Figure 3). As will be discussed later, a linear stability analysis of steady planar wave propagation through a uniform cell distribution in this model predicts that the waves are unstable to perturbations in the direction transverse to that of propagation. The authors interpret this as incipient stream formation.

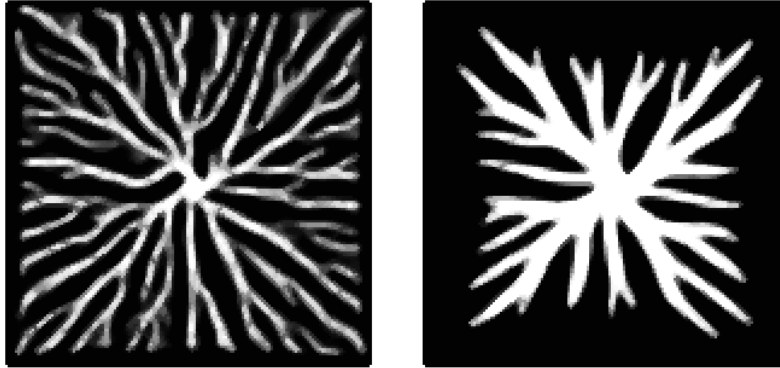


FIG. 3. *Two examples of the aggregation patterns produced by the model of Höfer et al. [11]. (From [10], with permission.). The computational scheme is based on an ADI splitting for diffusion, first-order explicit upwinding for the chemotaxis terms, and an explicit Euler step for the reaction terms. The results shown are at $t = 80$ minutes (left) and $t = 140$ minutes (right).*

A major problem concerning flux equations such as (3.2), (3.5), or the form used to obtain (3.6), is how one incorporates the microscopic responses of individual cells into the continuum level description of taxis contained in the chemotactic sensitivity. The analogous problem has been solved in simple cases in fluid mechanics, but to date little progress has been made on this problem in the biological context. One approach to this problem that incorporates more of the microscopic details builds on the kinetic theory approach used earlier [24, 1, 21]. This approach will be described later, but first we discuss a discrete cell description of aggregation in which movement is governed by internal variables.

3.2. A cell-based model for aggregation. The alternative to the continuum approach is to base a model on discrete cells with internal dynamics that describe signal transduction, the choice of direction, and movement in response to stimuli. Enough is known about the first two components to formulate detailed models, such as the one for signal transduction described earlier, but our knowledge of the biochemical control of movement is still too sketchy to warrant detailed models, and thus this step must be described by formal rules rather than mechanistically. Of course other steps such as cAMP secretion could also be described by formal rules, and the early models developed by Parnas and Segel [23] and by MacKay [15] are examples of this approach. These models are similar in that in each the cells are treated as black boxes which output a fixed amount of cAMP when stimulated. Diffusion of cAMP is taken into account, but there is no description of signal transduction, cAMP production, or adaptation in these models. The model of Parnas and Segel is in one space dimension and can effectively only address the question of how the cell decides when

to move. MacKay's model is formulated in two space dimensions and it can reproduce the observed streaming patterns and the effect of two competing pacemakers, and it produces spiral waves for suitable initial cell distributions. These models represent a first step in the modeling of aggregation, but the rules for cAMP production and secretion are formal and do not incorporate present experimental knowledge about these processes.

A model in which cells are treated as discrete units with internal variables and cAMP₀ is described by a continuum reaction-diffusion equation has recently been developed [4]. A detailed description of signal transduction and cAMP dynamics is incorporated into this model, and movement rules based on the intracellular dynamics can be explored. The model comprises two main parts: (i) the mechanism for signal transduction and cAMP relay response, for which the model described earlier is used, and (ii) the cell movement rules. The equations for the intracellular dynamics of the i^{th} cell are given by the first four equations in (2.1), and these can be written as the system

$$(3.9) \quad \frac{d\mathbf{w}^i}{d\tau} = \mathbf{G}^i(\mathbf{w}^i, C_o).$$

Here \mathbf{w}^i is a four-component vector wherein $w_4 \equiv C_i$. Variations of parameters from cell to cell can be incorporated by changing the \mathbf{G}^i . The evolution of the extracellular cAMP is governed by

$$(3.10) \quad \frac{\partial C_o(\mathbf{x}, \tau)}{\partial \tau} = \Delta_1 \nabla^2 C_o(\mathbf{x}, \tau) - \hat{\gamma}_9 \frac{C_o(\mathbf{x}, \tau)}{C_o(\mathbf{x}, \tau) + \gamma_8} + \sum_{i=1}^N \frac{V_c}{V_o} \delta(\mathbf{x} - \mathbf{x}_i) \left(sr(w_4^i) - \gamma_7 \frac{C_o(\mathbf{x}, \tau)}{C_o(\mathbf{x}, \tau) + \gamma_6} \right).$$

The position of the i^{th} cell is denoted \mathbf{x}_i , the first term represents diffusion of cAMP, the second represents the degradation of cAMP by extracellular phosphodiesterase, and the summation represents the localized sources and sinks of cAMP at the cells. The definition of the parameters is given in [4].

The other component of the model involves the cell movement rules, which determine when motion is initiated, how the direction is determined, and how long movement persists. It is known that locomotion and orientation are controlled separately in Dd [38], and thus we make the simplest hypothesis for the directional choice, namely that a cell moves in the direction of the local cAMP gradient when motion ensues. This does *not* require that the cell measure the gradient, but only that the orientation is determined, for example, by an intracellular gradient set up by the extracellular signal. Using the signal transduction scheme described earlier, Dallon and Othmer [3] show that an intracellular gradient can be established on the space and time scales that characterize signaling between cells in early aggregation. The other requirements of the movement model are to determine when movement is initiated and how long it persists. Various rules

have been explored in Dallon and Othmer [4], and as is shown there, formal rules based on a fixed duration of movement can produce aggregation. That is, a sort of ballistic movement in which cells ignore the environment for the duration of movement can be successful if the time is chosen properly, but if the duration is too short aggregation does not occur. However, by adding other mechanisms, such as directional persistence, aggregation can be restored [4].

However such formal rules are biologically unrealistic, because there is no coupling between the intra- or extracellular environment and the duration of movement. For example, if the profile of the cAMP wave is altered due to changes in the number of pacemakers that initiate a wave, a rule based on fixed durations could predict that cells continue to move after the wave has passed. In reality the choice of duration is undoubtedly determined by one or more intracellular variables, and an outline of a detailed model of how cells might choose the direction of motion and the length of a ‘run’ will be described later. Such a model has not been analyzed as yet, and it would probably be computationally prohibitive to include it in the simulations described later at present. Instead, more realistic rules based on internal variables were developed as follows [4]. It is known that in addition to activating the cAMP production pathway, cAMP also activates the production of another intracellular messenger, cyclic guanosine monophosphate (cGMP), [19]. It is also known that cGMP is near the beginning of the chemotactic response pathway, and that cGMP production adapts to the cAMP stimulus on a time scale of about 10-15 seconds. If cGMP adapts to extracellular cAMP levels then downstream components of the chemotactic response pathway will also adapt, perhaps on a longer time scale, except in unusual circumstances. Thus it is assumed in the model that there is a downstream ‘motion controller’, the identity of which is not known. This species must control the motion in such a way that the cell moves only when cAMP is increasing, because, as noted earlier, it is known that wild-type cells only move in the rising phase of the cAMP wave. In the model we used as a stand-in a quantity in the cAMP pathway that has the appropriate time course. This biochemically-based rule is more realistic than the *ad hoc* rules.

The algorithm we developed to solve these equations can be summarized as follows [4]. Given an initial cell distribution for 10-80K cells (which may be uniformly or randomly-istributed in 2D), and the initial distribution of extracellular cAMP, we perform the following steps.

- Solve for the extracellular cAMP at time t^{n+1} on a regular grid, using ADI for the PDE, but evaluating the secretion term at t^n .
- Interpolate the cAMP from the grid to the cell positions and update the intracellular variables by an implicit scheme.
- Update cell movement. If a cell is not moving, should it begin to move? If so, compute the direction and start the motion. If it is moving, check to see if it should continue moving.

- Transfer the secreted cAMP to the grid and repeat the cycle.

To solve the extracellular equation (3.10), the Laplace operator is discretized using fourth order centered differences, the reaction term is lagged in time, and the resulting equations are solved using the Peaceman-Rachford ADI method [25]. The internal variables are updated using the trapezoidal method. The interpolation from grid to cell is a tensor product interpolant using quartic Lagrangian interpolation in each direction [26]. The grid discretization h is equal in the x and y directions and therefore this interpolator has an error proportional to h^5 . Except for the error in the interpolation from cell to grid, the scheme has a local truncation error of $O(kh^4)$. The interpolation from the cell to the grid is a tensor product interpolation which is continuous, bivariate and piecewise linear. It was defined to approximate the Dirac distribution as the spatial grid size approaches zero.

Two additional modifications, cell stacking and cell adhesion, are included in the algorithm in order to improve computational efficiency. A typical aggregation field is 1 cm^2 , and cell densities range from 2.5×10^4 cells/cm² to 10^6 cells/cm². In the first modification we allow each cell to represent an integer number of cells, typically between 2 and 16. This means that the reaction contribution in (3.10) is multiplied by the number of stacked cells and the input-output characteristics of the model are maintained; the effect is that there are fewer but stronger sources of cAMP. One argument which suggests that this should not affect the results significantly is that the interpolation from cells to the grid for four evenly-spaced cells within one grid square is the same as four stacked cells located at the center of the grid. Computational experiments verify that stacking the cells does not significantly alter the results [4]. As may be expected, for larger cell stacking the simulations show that the aggregation patterns are more compact, but qualitatively the results remain similar.

The addition of cell adhesion improves the computational efficiency, but also has a biological motivation. When cells come in contact with one another they adhere via membrane binding proteins [31], and to incorporate this in the model, when the centers of two or more cells lie within 5 microns of each other they are all combined to form one cell. The new cell is at the location of one of the combined cells and its contribution to the cAMP concentration is multiplied by the number of cells combined. This only changes the results of the model in minor ways.

Simulations of the model produce results which match very well with experimental results (cf. Figure 4(a)). The biochemically-based rule shows how a cell can respond to temporally-increasing cAMP levels by predicating motion on a threshold of an intracellular variable, and it also solves the ‘back-of-the-wave’ problem, in that a cell does not respond to the receding cAMP wave after it passes, even though it sees a positive gradient on the back side of the wave. These simulation results support the conclusion reached by Soll *et al.* [32], that cells seem to orient during the beginning

of the cAMP wave of and then maintain their direction. When there are many pacemakers the aggregation field breaks up into a number of smaller fields, although certainly not equal in number to the number of pacemakers present (cf. Figure 4(b)), as is observed experimentally. These computations show that single cells can be pacemakers, in agreement with earlier theoretical analysis [5], but they also show that many of these pacemakers will be entrained by others. Whether or not an individual pacemaker can continue to oscillate in the face of periodic signals from other sources is a function of how large an aggregate it has recruited, and hence how strong a signal it emits, differences between its frequency and that of other sources, and the initial distribution of cells. As yet there is no theoretical analysis that enables one to predict when it will survive, but it is an important question because the answer would shed light on the breakup of waves by pacemakers and hence on the origin of spirals.

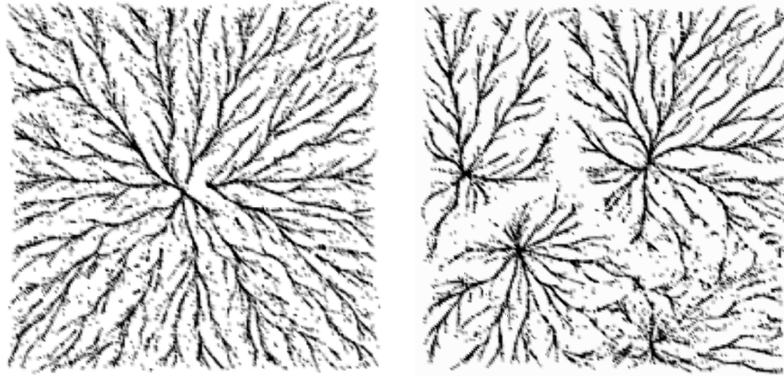


FIG. 4. *Two examples of the aggregation patterns produced by the discrete cell model. In (a) cell movement is governed by an internal variable that adapts and in (b) there are 0.1% pacemakers randomly-placed in the aggregation field initially and cells move according to the rules in (a). Both patterns are shown at 150 minutes, the domain is 1 centimeter by 1 centimeter with 200 grid points in each direction, and the number of cells used corresponds to a volumetric density of about 0.2. (After Dallon and Othmer [4].)*

3.3. Continuum descriptions from microscopic rules. A question raised earlier is how one can incorporate detailed microscopic descriptions of movement such as were described in the previous section into a macroscopic quantity such as the chemotactic sensitivity. A general description of a random walk governed by a semi-Markov process in which the walker executes jumps in space leads to a renewal equation of the form

$$(3.11) \quad P(\mathbf{x}, t|0) = \hat{\Phi}(t)\delta(\mathbf{x}) + \int_0^t \int_{R^n} \phi(t - \tau)T(\mathbf{x}, \mathbf{y})P(\mathbf{y}, \tau|0) dy d\tau.$$

for the probability $P(\mathbf{x}, t|0)$ that a walker beginning at the origin at $t = 0$ is at position \mathbf{x} at time t [21]. It is shown in [21] that the evolution of $P(\mathbf{x}, t|0)$ is governed by a diffusion equation for suitable choices of the waiting time distribution ϕ (which determines the distribution $\hat{\Phi}(t)$) and the jump kernel $T(\mathbf{x}, \mathbf{y})$. Chemotaxis can be incorporated in this approach, but an alternative stochastic process that may be more appropriate for describing the motion of Dd cells than the space jump process that leads to (3.11) is called the velocity-jump process [1, 21]. In this process the velocity, rather than the position changes at random times, which is more appropriate for describing the motion of amoeboid cells such as Dd because they change their direction and speed in the presence of stimuli [6], but do not make instantaneous jumps in space. As we indicated earlier, the directional changes are not randomly chosen, but rather, are chosen so as to align the cell with the direction of the stimulus. In the following paragraphs we sketch a formulation that is sufficiently general to include these behaviors, as well as the involvement of internal cell variables, in the description of motion. Details are given elsewhere [21, 20].

We suppose that in the absence of noise due to molecular fluctuations, the internal variables involved in signal detection, transduction, processing and response are described by the deterministic system

$$(3.12) \quad \frac{d\mathbf{c}}{dt} = \mathbf{g}(\mathbf{c}, C_0),$$

where \mathbf{c} is a vector of m internal variables and C_0 is the chemotactic substance. In the model described earlier (cf 2.1), there are four internal concentration variables in the cAMP transduction pathway, and C_0 is extracellular cAMP. However, as we indicated earlier, to describe control of motion in chemotaxis one would have to use a model such as that developed in [37] for the cGMP pathway. The form of this system can be very general but it should always have the ‘adaptive’ property that the steady-state value of the appropriate internal variable (the ‘motion controller’) is independent of the stimulus, and that the steady state is globally attracting with respect to the positive cone of R^m . A simple model which captures some of the essential features of an adaptive system is given in OS.

To introduce the phase-space description of motion, let $p(\mathbf{x}, \mathbf{v}, \mathbf{c}, t)$ be the density function for individuals in a $2n + m$ -dimensional phase space with coordinates $(\mathbf{x}, \mathbf{v}, \mathbf{c})$ where \mathbf{v} , which takes values in R^n , is the velocity. Then $p(\mathbf{x}, \mathbf{v}, \mathbf{c}, t) d\mathbf{x} d\mathbf{v} d\mathbf{c}$ is the number density of individuals with position between \mathbf{x} and $\mathbf{x} + d\mathbf{x}$, velocity between \mathbf{v} and $\mathbf{v} + d\mathbf{v}$, and internal state between \mathbf{c} and $\mathbf{c} + d\mathbf{c}$. The quantity

$$(3.13) \quad \rho(\mathbf{x}, t) = \int p(\mathbf{x}, \mathbf{v}, \mathbf{c}, t) d\mathbf{v} d\mathbf{c}$$

is the density of individuals at \mathbf{x} , whatever their velocity and internal state. If we neglect external forces such as gravity then the evolution of p is

governed by the partial differential equation

$$(3.14) \quad \frac{\partial p}{\partial t} + \nabla_{\mathbf{x}} \cdot \mathbf{v}p + \nabla_{\mathbf{c}} \cdot \dot{\mathbf{c}}p = \mathcal{R},$$

where \mathcal{R} is the rate of change of p due to the random choice of velocity.

Since Dd amoeba modify the chemotactic field when they relay the signal, one has to augment (3.12) by an evolution equation for C_0 . If transport is only via diffusion then this equation takes the form

$$(3.15) \quad \frac{\partial C_0}{\partial t} = D\Delta C_0 + f(\rho(\mathbf{x}, t), \mathbf{c}, C_0).$$

In general \mathcal{R} can contain both a diffusive and a jump component, but here we only include the latter, and we assume that the jump contribution arises from a Poisson process that generates random velocity changes. In the absence of noise the internal state evolves according to (3.12), and consequently (3.14) becomes

$$(3.16) \quad \begin{aligned} \frac{\partial p}{\partial t} + \nabla_{\mathbf{x}} \cdot \mathbf{v}p + \mathbf{g} \cdot \nabla_{\mathbf{c}}p = \\ - \lambda p - (\nabla_{\mathbf{c}} \cdot \mathbf{g})p + \lambda \int T(\mathbf{v}, \mathbf{v}')p(\mathbf{x}, \mathbf{v}', t) d\mathbf{v}'. \end{aligned}$$

Here λ is the intensity of the Poisson process, λ^{-1} is the mean run length time between the random choices of direction, and the kernel $T(\mathbf{v}, \mathbf{v}')$ gives the probability of a change in velocity from \mathbf{v}' to \mathbf{v} , given that a reorientation occurs. $T(\mathbf{v}, \mathbf{v}')$ is non-negative and normalized so that $\int T(\mathbf{v}, \mathbf{v}') d\mathbf{v} = 1$.

This equation shows that the dependence on the internal state adds both a drift term with velocity \mathbf{g} and a source or sink of strength $\nabla_{\mathbf{c}} \cdot \mathbf{g}$. Since \mathbf{g} depends on the stimulus $C_0(\mathbf{x})$, this velocity and source strength depend explicitly on the spatial position, but this phase-space description is still too simple to describe the motion of Dd. Firstly, it is convenient to distinguish between moving and stationary cells, *i. e.*, between $\mathbf{v} = 0$ and $\mathbf{v} \neq 0$ in (3.16), since otherwise the intensity λ depends explicitly on the velocity. After this splitting we suppose that λ is independent of the velocity, but for Dd λ decreases slightly when the cell moves upgradient [6]¹. Under this hypothesis one can show that the resulting jump process is a Markov process.

A second simplification is to assume that there are only two speeds, which can be taken as 0 and s , and that the motion is restricted to two

¹Recent data suggest that this is an oversimplification; cells do not choose new directions via a Poisson process. Instead there appears to be an intrinsic periodicity to the extension of pseudopods, at least in unstimulated amoeba [13, 29]. Such behaviors can be taken into account by introducing other state variables, but we do not pursue this here.

space dimensions. Let $p_1(\mathbf{x}, \phi, \mathbf{c}, t)$ be the density of cells moving in the direction ϕ , and let $p_0(\mathbf{x}, \phi, \mathbf{c}, t)$ be the density of stationary cells whose direction was ϕ when they stopped. Further, let λ_{10} denote the rate at which moving cells stop, let λ_{01} denote the rate at which cells begin to move, and let λ_{11} denote the rate of direction changes amongst moving cells. The resulting equations have the form

$$(3.17) \quad \frac{\partial p_1}{\partial t} + s\xi \cdot \nabla_{\mathbf{x}} p_1 + \nabla_{\mathbf{c}} \cdot \mathbf{g} p_1 = -\lambda_{10} p_1 + \lambda_{01} \int T_0(\phi, \phi') p_0(\mathbf{x}, \phi', t) d\phi' \\ - \lambda_{11} p_1 + \lambda_{11} \int T_1(\phi, \phi') p_1(\mathbf{x}, \phi', t) d\phi'.$$

$$(3.18) \quad \frac{\partial p_0}{\partial t} + \nabla_{\mathbf{c}} \cdot \mathbf{g} p_0 = \lambda_{10} p_1 - \lambda_{01} \int T_0(\phi, \phi') p_0(\mathbf{x}, \phi', t) d\phi',$$

One objective in studying these equations is to determine whether there is an asymptotic regime in which the flux of cells reduces to an equation of the form (3.2). For this purpose one must postulate how the coefficients λ_{ij} and the kernels T_i depend on the internal state, and through them, on the external cAMP field. The choice which leads to the rules used in [4] is $\lambda_{11} = 0$ (cells maintain the direction they choose when movement begins), λ_{10} and λ_{01} either zero or infinity, depending on the level of the motion controller, and the kernel T_0 a Dirac distribution with mass at the angle corresponding to the local cAMP gradient. Work on the analysis of the more general form of the equations is in progress.

4. The origin of streaming. The formation of streams is a prominent feature of aggregation in low-density fields, and in this section we discuss the mechanisms suggested by different models to explain their origin. In Figure 5 we show the distribution of cells at two times. It is clear in the right panel that the streams first develop close to the pacemaker and then grow outward. Also noteworthy is the branching pattern of the streams, and in particular, that there is no dominant length scale in the pattern: it contains a broad spectrum of length scales and may be approximately fractal over a limited range of scales.

A heuristic argument which suggests that the spatially-uniform cell distribution should be unstable to sufficiently large disturbances goes as follows. Cells move in the direction of higher cAMP and produce it as well; therefore a disturbance that creates a large enough density or cAMP nonuniformity will induce cell movement and this will in turn reinforce the nonuniformity. Moreover, the variations in density or concentration will be reinforced with each passing cAMP wave. Thus there is little doubt that large variations in density can lead to streaming; where current theories differ is whether the uniform density distribution is stable or unstable to small disturbances, and whether or not the streams first originate near

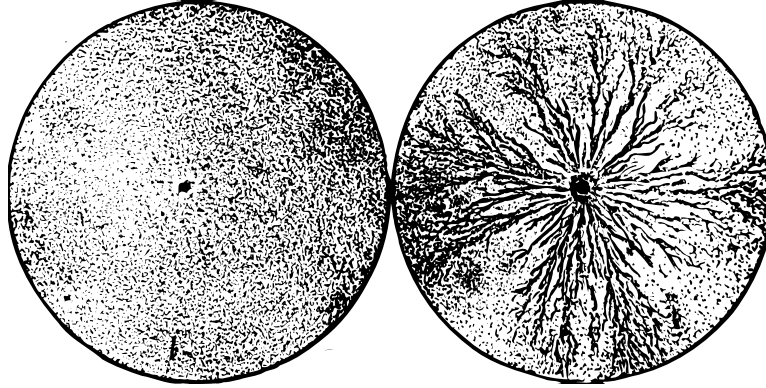


FIG. 5. *The evolution of streams during aggregation. The left panel shows an early, relatively-uniform field with a pacemaker at the center, and the right panel shows the development of streams at a later stage. Note that the streams are most pronounced near the pacemaker, and that there is little stream formation near the boundary of the dish. (From Raper [28].)*

the center or near the outer boundary. The experimental evidence clearly suggests that they originate near the center.

Computational evidence that a perfectly uniform initial distribution of identical cells will not develop significant streams is given in [4]. There it was shown that when edge effects are eliminated by identifying two sides of the domain and signaling is via a plane wave, no instabilities transverse to the direction of propagation develop during the first 100-150 minutes. This lead to the conjecture that streaming on the observed time scale requires a sufficiently large initial variation in either the cell density or cAMP, *i.e.*, it is due to a finite-amplitude instability. Here we provide further evidence in support of this conjecture by comparing the evolution of an initially-uniform field driven by a central pacemaker with that for an initially-random density distribution. In Figure 6 we show the cell density at two fixed times on two distinct circles centered at the pacemaker². In the top left panel one sees that at $r = 0.2$ the dominant fluctuations are of amplitude 1.0 unit around a mean of 10, and a much smaller fluctuation about a lower mean at $r = 0.4$ (the mean is lower at $r = 0.4$ than at $r = 0.2$,

²Details of how the simulations are done can be found in [4]: suffice it to say here that for this figure we begin with all cells distributed uniformly on the grid points and we allow the system to evolve according to the algorithm described earlier. We record the entire state (intracellular variables, cell positions and extracellular cAMP) at fixed intervals. To obtain the densities shown in Figure 6 we interpolate the cell densities to the uniform grid, and then to equally-spaced points on the desired circle. We use an FFT algorithm to obtain the power spectrum shown in Figure 7. We use 100 points on each circle, which on the inner circle gives roughly one half the largest meaningful frequency for the underlying computational grid. One could use twice as many points on the outer circle, but we have not done this.

but higher than the initial mean of 8, which reflects the fact that cells are moving inward.)³ At a later time (bottom panel) the variation around the

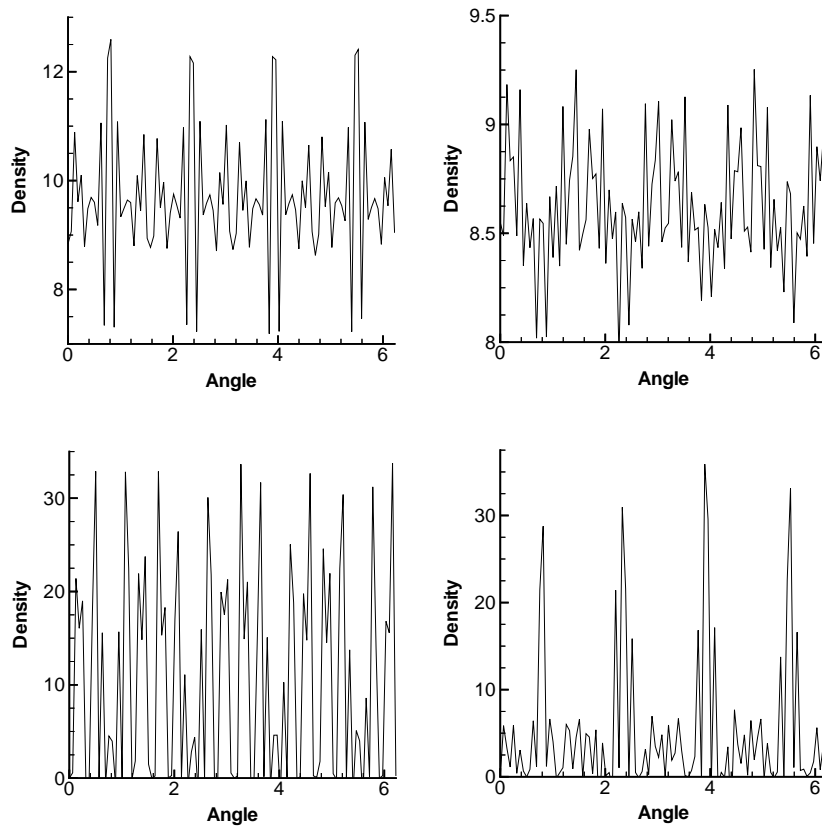


FIG. 6. Cell densities around a circle of radius 0.20 (left) and radius 0.40 (right) at 100 minutes (top) and 280 minutes (bottom). The initial cell distribution was uniform and equal to 8.

circle is larger, indicating that some streaming has developed, particularly near the center. Further insight can be gotten from the power spectrum on the circles, as is shown in Figure 7. The θ -independent component, which is of order 10, is not shown in this figure, but one sees that the amplitudes of all the variable components (which initially are all $\mathcal{O}(10^{-13})$) are relatively small compared to the constant component. The largest amplitude

³The larger-amplitude peaks lie along the diagonals centered at the pacemaker. The movement toward the diagonals results from the fact that the central pacemaker, which in the continuum formulation is a disk of radius 0.05 centimeters, is approximated by a square region that is rotated by 45° from the coordinate directions. This asymmetry can be reduced by using finer grids, but it cannot be eliminated on a Cartesian grid.

in the left panel corresponds to the peaks and sidebands associated with streams along the diagonal. In Figure 8 we show the cell tracks of cells that

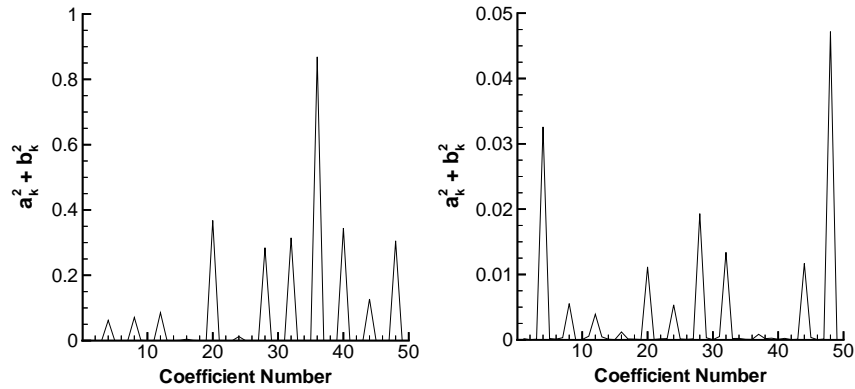


FIG. 7. The power spectrum of the density distributions at $t = 100$ for $r = 0.2$ (left) and $r = 0.4$ (right), represented by the sum of the squares of the amplitudes of the sine and cosine terms corresponding to the mode number on the abscissa.

begin on either of two circles: one sees there that the cells move essentially straight inward until they are close to the pacemaker. Near the boundary of the pacemaker there is a slight rotary motion.

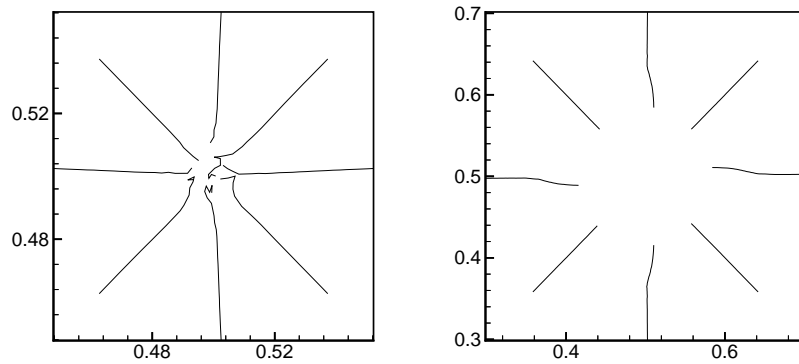


FIG. 8. The tracks of 8 cells initially on a circle of radius 0.05 (left) and 0.20 (right), for an initially-uniform cell distribution.

Next let us examine the evolution for an initially-random distribution. In Figure 9 we show the two-dimensional cell distributions at two fixed times for a random initial distribution of cells, and in Figures 10-12 we show

results analogous to those in Figures 6-8. Several conclusions emerge from these figures. Firstly it is clear that the small density variations that arise

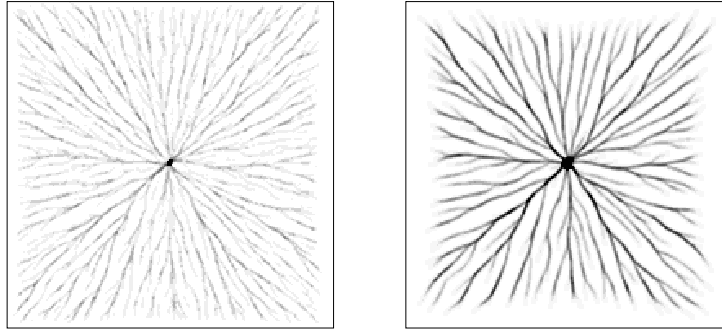


FIG. 9. The two-dimensional cell distribution at $t=100$ (left) and $t=280$ (right). The conditions are the same as in Figure 4, except that here $\gamma_2 = 0.35$ at the pacemaker, rather than 0.4.

from a random initial cell distribution lead to much faster development of streams than in the case of uniform initial conditions. A comparison of Figure 10 with Figure 6 at comparable times and distances from the pacemaker shows that the deviations from the average initial density under random initial conditions are much larger than those under uniform initial conditions. Perhaps more significant *vis a vis* stream formation is that there are significant regions of very low density in the case of random initial conditions, in contrast to the situation for uniform initial conditions. The power spectra shown in Figure 11 confirm the fact that streams grow more rapidly starting from a random initial density, and the cell tracks shown in Figure 12 confirm that streams are more pronounced at equal times.

Figures 10 and 11 also shed light on the evolution of stream development in the model. A comparison of the spectra at $t = 100$ shows that there is significantly more 'energy'⁴ in nonuniform modes at $r = 0.2$ than at $r = 0.4$. Furthermore, at $r = 0.2$ the energy is more localized in the high-frequency modes, which indicates a more rapidly-varying density distribution, as can also be seen in the density plots. This suggests that streams are initiated near the center and develop outwardly as time progresses. Thus the model predictions are in agreement with the experimental results in this regard, but they differ from conclusions reached by others using continuum models.

These results provide further support for the conjecture that finite-amplitude disturbances in density or cAMP concentration are needed to

⁴As measured by the sum of the squares over all modes. Of course the constant coefficient in the expansion is larger at $r = 0.2$ than at $r = 0.4$, which reflects the higher average density at $r = 0.2$, but these coefficients are not shown in the figures.

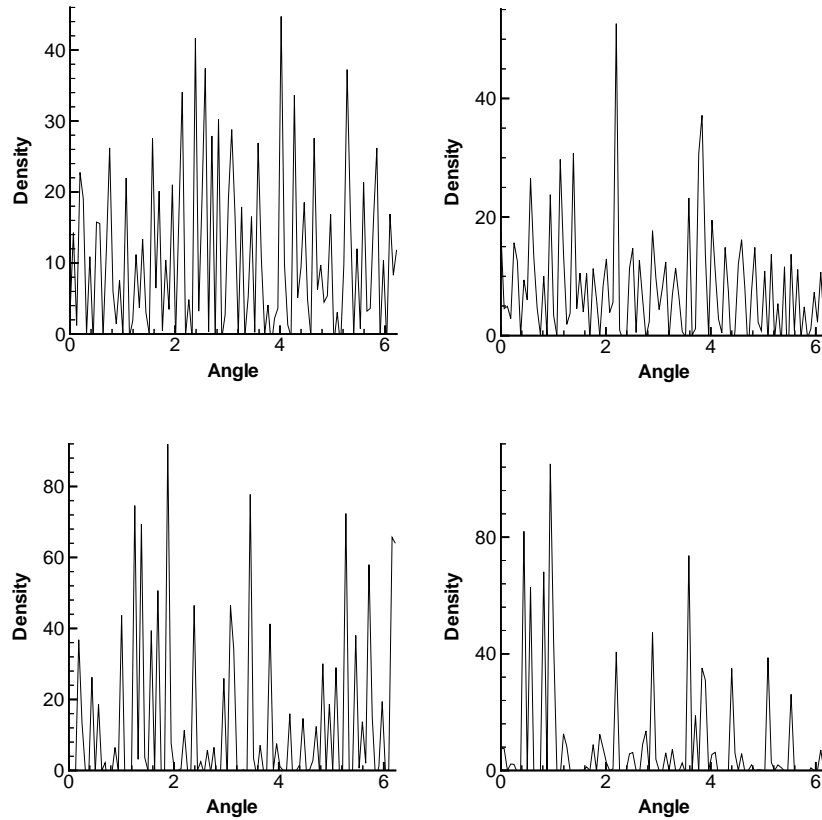


FIG. 10. The cell densities on circles of radius 0.20 (left) and 0.40 (right) at $t=100$ (top) and $t=280$ (bottom).

initiate streaming. Aside from the higher density along diagonals, which is due to the asymmetry noted earlier, the density variation of an initially-uniform field along the circle of radius 0.2 is less than 10% at 100 minutes, and although there is more variation by 280 minutes, there is no dominant wavelength, as would be expected in a linearly unstable system. By comparison, when the initial distribution is random the density varies over an order of magnitude or more at the same time (*cf.* Figure 10). In addition, the cell tracks in an initially uniform field show that cells move inward essentially along rays until they are close to the pacemaker region, whereas the tracks are curved significantly for the random initial distribution. Finally, if there were a linear instability of the cAMP wavefront one would expect disturbances to grow as the wave propagates outward. This would lead to the prediction that the amplitude of the azimuthal variation

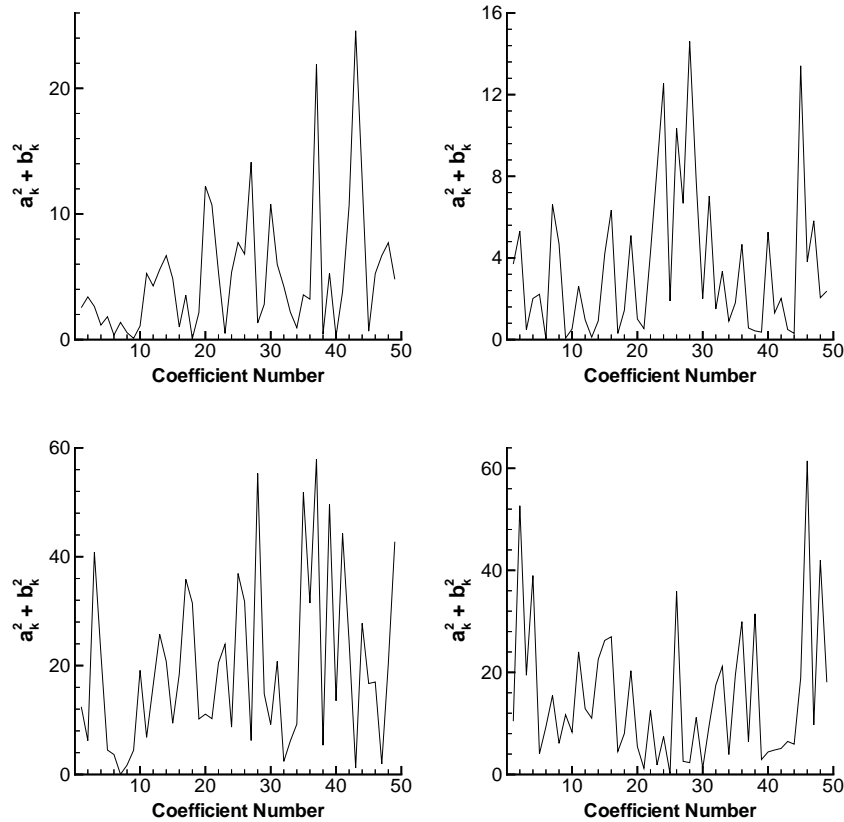


FIG. 11. The power spectra corresponding to the density profiles in Figure 10.

in cAMP is greatest at the outer boundary, which in turn would lead to initiation of streaming at the outer boundary of the domain, contrary to what is observed.

There are several reasons why the uniform distribution should be stable to small disturbances. Firstly, it is known that there is a small diffusional component to cell motion, and this will tend to damp small density disturbances. Although diffusion is not explicitly included in the model, it can be shown that the numerical procedure introduces it via the truncation errors. It is also known that the transduction pathway to the locomotory machinery adapts to the extracellular cAMP signal, and this fact is included in the model used here. As a result of adaptation, disturbances that vary slowly over time will not be amplified by cell movement. Finally, there is a threshold in the cAMP gradient of $\sim 10 \text{ nM/mm}$ [7] below which the cells do not chemotact. These three factors, diffusion, adaptation and a threshold, all

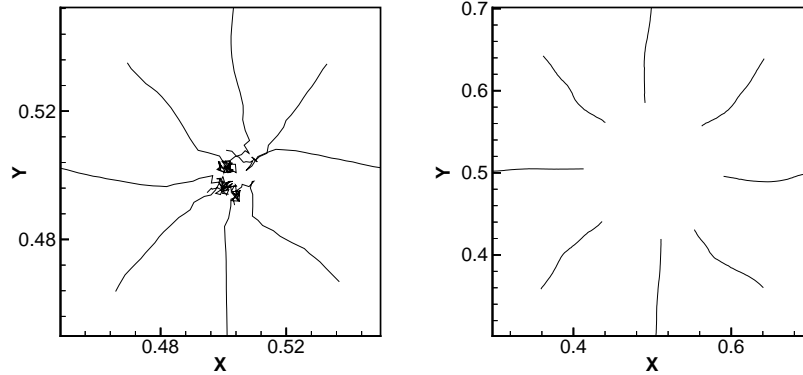


FIG. 12. The tracks of 8 cells initially on a circle of radius 0.05 (left) and 0.20 (right) for a random initial cell distribution.

mitigate against amplification of small disturbances, and it is conjectured in [4] that the streams result from a finite-amplitude instability.

Nanjundiah [17] carries out a stability analysis of the Keller-Segel system on a circular domain with a steady signaling center and finds unstable “azimuthal” modes which he links to the occurrence of cell streaming. However the central core of cells in Nanjundiah’s analysis is a steady source of cAMP and there are no propagating waves. While this analysis may apply in systems that do not use an oscillatory core, it does not apply to Dd. Levine and Reynolds [14] find that for a different model streaming is due to a linear instability in the governing equations. These authors use a continuum description and show that planar traveling waves can be unstable to perturbations of wavelength greater than approximately 8 mm, but stable otherwise. They conclude that a streaming instability can occur, but their results show that it is a very long wavelength instability and thus would probably not be seen on the scale of normal aggregation patterns. Moreover, in the mechanism they suggest the growing modes are not stationary in space, but rather, they propagate outward with the cAMP waves as their amplitude increases. Thus the largest spatial variations in density and cAMP will be seen at the outer boundary of the domain, which implies that streams will grow most rapidly near the outer boundary. However, as Figure 5 shows, streams are most prominent near the pacemaker in early aggregation.

Vasiev *et al.* [41], who also use a continuum model for the cell density, conclude that a necessary condition for the development of streams is that the initial density be nonuniform. However, they did not address the question as to whether or not the uniform distribution is stable to small amplitude disturbances. These authors suggest that the major factor in

stream formation is a change in the speed of the cAMP wave as density varies, and this may be an important factor. Höfer and Maini [10] incorporate this idea and the curvature-velocity relationship for nonplanar waves into a simplified model on which some analysis can be done. They also conclude that plane cAMP waves can become unstable to transverse perturbations, but as in the Reynolds-Levine analysis, the disturbances propagate outward as they grow, and thus the largest amplitude will be seen on the outer boundary.

In conclusion, the existing simplified continuum models make predictions that are at variance with both the experimental observations and with the computational results obtained using a discrete cell model. The discrete-cell model already incorporates details of the individual cell behavior, but further work is needed to incorporate into a continuum model a description of how the onset and duration of motion is controlled and the cell-cell interactions that occur at higher densities. One approach to this was sketched out in the previous section. Moreover the continuum analyses cited are based on linearized equations, but nonlinear effects may alter the conclusions reached from those analyses, and thus a genuinely nonlinear analysis is needed. Analysis of continuum models that incorporate more internal details might show that there is a finite-amplitude instability, rather than the linear instabilities found in these models to date.

REFERENCES

- [1] W. ALT, *Biased random walk models for chemotaxis and related diffusion approximations*, Journal of Mathematical Biology, 9 (1980), pp. 147–177.
- [2] J. T. BONNER, *The Development of Dictyostelium*, Academic Press, 1982, ch. Comparative Biology of Cellular Slime Molds, pp. 1–33.
- [3] J. DALLON AND H. G. OTHMER, *A continuum analysis of the chemotactic signal seen by Dictyostelium discoideum*, J. Theor. Biol., 194 (1998), pp. 461–483.
- [4] J. C. DALLON AND H. G. OTHMER, *A discrete cell model with adaptive signalling for aggregation of dictyostelium discoideum*, Philosophical transactions of the Royal Society of London Series B, Biological sciences, 352 (1997), pp. 391–417.
- [5] G. DEYOUNG, P. B. MONK, AND H. G. OTHMER, *Pacemakers in aggregation fields of Dictyostelium discoideum. Does a single cell suffice?*, Journal of Mathematical Biology, 26 (1988), pp. 486–517.
- [6] P. FISHER, R. MERKL, AND G. GERISCH, *Quantitative analysis of cell motility and chemotaxis in Dictyostelium*, Journal of Cell Biology, 92 (1989), pp. 807–821.
- [7] P. R. FISHER, *Pseudopodium activation and inhibition signals in chemotaxis by Dictyostelium discoideum amoebae*, Cell Biol., 1 (1990), pp. 87–97.
- [8] P. FOERSTER, C. MÜLLER, AND B. HESS, *Curvature and spiral geometry in aggregation patterns of Dictyostelium discoideum*, Development (Cambridge), 109 (1990), pp. 11–16.
- [9] A. R. GINGLE AND A. ROBERTSON, *The development of the relaying competence in Dictyostelium discoideum*, Journal of Cell Science, 20 (1976), pp. 21–27.
- [10] T. HÖFER AND P. MAINI, *Streaming instability of slime mold amoebae: An analytical model*, Phys. Rev. E, 56 (1997), pp. 1–7.
- [11] T. HOFER, J. A. SHERRATT, AND P. K. MAINI, *Dictyostelium discoideum: cellular self-organization in an excitable biological medium*, Proc R Soc Lond B Biol Sci (PXF), 259 (1995), pp. 249–257.

- [12] E. F. KELLER AND L. A. SEGEL, *Conflict between positive and negative feedback as an explanation for the initiation of aggregation in slime mould amoebae*, *Nature*, 227 (1970), pp. 1365–1366.
- [13] T. KILLICH, P. J. PLATH, X. WEI, H. BULTMANN, L. RENSING, AND M. G. VICKER, *The locomotion, shape and pseudopodial dynamics of unstimulated Dictyostelium cells are not random*, *Journal of Cell Science*, 106 (1993), pp. 1005–1013.
- [14] H. LEVINE AND W. REYNOLDS, *Streaming instability of aggregating slime mold amoebae*, *Phys. Rev. Letts.*, (1991), pp. 2400–2403.
- [15] S. A. MACKAY, *Computer simulation of aggregation in Dictyostelium discoideum*, *Journal of Cell Science*, 33 (1978), pp. 1–16.
- [16] J. L. MARTIEL AND A. GOLDBETER, *A model based on receptor desensitization for cyclic AMP signalling in Dictyostelium cells*, *Biophysical Journal*, 52 (1987), pp. 807–828.
- [17] V. NANJUNDIAH, *Chemotaxis, signal relaying and aggregation morphology*, *Journal of Theoretical Biology*, 42 (1973), pp. 63–105.
- [18] P. C. NEWELL, *Attraction and adhesion in the slime mold dictyostelium*, in *Fungal Differentiation: A Contemporary Synthesis*, J. E. Smith, ed., Marcel Dekker, Inc., New York, NY, USA, 1983, pp. 43–71.
- [19] P. C. NEWELL, G. N. EUROPE-FINNER, G. LIU, B. GAMMON, AND C. A. WOOD, *Chemotaxis of Dictyostelium discoideum: The signal transduction pathway to actin and myosin*, in *Biology of the Chemotactic Response*, J. P. Armitage and J. M. Lackie, eds., Cambridge University Press, 1990, pp. 241–272.
- [20] H. G. OTHMER, *A model for chemokinesis and chemotaxis with internal state and adaptation*. In preparation, 1999.
- [21] H. G. OTHMER, S. R. DUNBAR, AND W. ALT, *Models of dispersal in biological systems*, *Journal of Mathematical Biology*, 26 (1988), pp. 263–298.
- [22] H. G. OTHMER AND P. SCHAAP, *Oscillatory cAMP signaling in the development of Dictyostelium discoideum*. *Comments on Theor. Biol.*; To appear, 1997.
- [23] H. PARNAS AND L. A. SEGEL, *Computer evidence concerning the chemotactic signal in Dictyostelium discoideum*, *Journal of Cell Science*, 25 (1977), pp. 191–204.
- [24] C. S. PATLAK, *Random walk with persistence and external bias*, *Bull. of Math. Biophys.*, 15 (1953), pp. 311–338.
- [25] D. W. PEACEMAN AND H. H. RACHFORD, JR., *The numerical solution of parabolic and elliptic differential equations*, *J. Soc. Indust. Appl. Math*, 3 (1955), pp. 28–41.
- [26] A. RALSTON AND P. RABINOWITZ, *A First Course in Numerical Analysis*, McGraw Hill Book Company, New York, 1978.
- [27] R. K. RAMAN, Y. HASHIMOTO, M. H. COHEN, AND A. ROBERTSON, *Differentiation for aggregation in the cellular slime molds: The emergence of autonomously signalling cells in Dictyostelium discoideum*, *J. Cell. Sci.*, 21 (1976), pp. 243–259.
- [28] K. B. RAPER, *The Dictyostelids*, Princeton University Press, Princeton, NJ, USA, 1984.
- [29] A. D. SHENDEROV AND M. P. SHEETZ, *Inversely correlated cycles in speed and turning in an ameba: An oscillatory model of cell locomotion*, *Biophysical Journal*, 72 (1997), pp. 2382–2389.
- [30] F. SIEGERT AND C. WEJER, *Digital image processing of optical density wave propagation in Dictyostelium discoideum and analysis of the effects of caffeine and ammonia*, *J. Cell Sci.*, 93 (1989), pp. 325–335.
- [31] C. H. SIU, *Cell-cell adhesion molecules in Dictyostelium*, *BioEssays*, 12 (1990), pp. 357–362.
- [32] D. R. SOLL, D. WESSELS, AND A. SYLWESTER, *The motile behavior of amoebae in the aggregation wave in Dictyostelium discoideum*, in *Experimental and Theoretical Advances in Biological Pattern Formation: Proceedings of a NATO Advanced Research Workshop on Biological Pattern Formation*, held August

- 27–31, 1992, in Oxford, England, United Kingdom, H. G. H. G. Othmer, P. K. Maini, and J. D. J. D. Murray, eds., vol. 259 of NATO ASI series. Series A, Life sciences, New York, NY, USA; London, UK, 1993, Plenum Press, pp. 325–338.
- [33] J. SWANSON AND D. L. TAYLOR, *Local and spatially coordinated movements in dictyostelium discoideum amoebae during chemotaxis*, Cell, 28 (1982), pp. 225–232.
- [34] Y. TANG AND H. G. OTHMER, *A G protein-based model of adaptation in Dictyostelium discoideum*, Mathematical Biosciences, 120 (1994), pp. 25–76.
- [35] Y. TANG AND H. G. OTHMER, *Excitation, oscillations and wave propagation in a G-protein-based model of signal transduction in Dictyostelium discoideum*, Philosophical transactions of the Royal Society of London Series B, Biological sciences, 349 (1995), pp. 179–??
- [36] K. J. TOMCHIK AND P. N. DEVREOTES, *Adenosine 3',5'-monophosphate waves in Dictyostelium discoideum: A demonstration by isotope dilution-fluorography*, Science, 212 (1981), pp. 443–446.
- [37] R. VALKEMA AND P. J. VAN HAASPERT, *A model for cAMP-mediated cGMP response in Dictyostelium discoideum*, Mol Biol Cell (BAU), 5 (1994), pp. 575–585.
- [38] B. VAN DUJIN AND P. J. VAN HAASPERT, *Independent control of locomotion and orientation during Dictyostelium discoideum chemotaxis*, Journal of Cell Science, 102 (1992), pp. 763–768.
- [39] B. VARNUM, K. B. EDWARDS, AND D. R. SOLL, *Dictyostelium amebae alter motility differently in response to increasing versus decreasing temporal gradients of cAMP*, Journal of Cell Biology, 101 (1985), pp. 1–5.
- [40] B. VARNUM AND D. R. SOLL, *Effects of cAMP on single cell motility in Dictyostelium*, Journal of Cell Biology, 99 (1984), pp. 1151–1155.
- [41] B. N. VASIEV, P. HOGEWEG, AND A. V. PANFILOV, *Simulation of Dictyostelium discoideum aggregation via reaction-diffusion model*, Physical Review Letters, 73 (1994), pp. 3173–??
- [42] D. WESSELS, J. MURRAY, AND D. R. SOLL, *Behavior of Dictyostelium amoebae is regulated primarily by the temporal dynamic of the natural cAMP wave*, Cell Motility and the Cytoskeleton, 23 (1992), pp. 145–156.